Is the Avoided Crossing State a Good Approximation for the Transition State of a Chemical Reaction? An Analysis of Menschutkin and Ionic S_N2 Reactions

S. Shaik,*[1a,b] A. Ioffe,[1b,c] A. C. Reddy,[1b] and A. Pross[1d,e]

Contribution from the Department of Organic Chemistry and the Fritz Haber Center of Molecular Dynamics, The Hebrew University, 91904 Jerusalem, Israel, and the School of Chemistry, The University of Sydney, NSW 2006, Australia

*Received July 19, 1993. Revised Manuscript Received October 20, 1993**

Abstract: This paper outlines a new approach for characterizing the transition state (TS) of a chemical reaction by introducing the concept of an avoided crossing state (ACS). The ACS (defined by eq 1) is a well-defined point on the reaction surface in the immediate vicinity of the TS and therefore may be used as a TS model. The key property of the ACS is that reactant and product Heitler-London configurations contribute equally to its wave function, and as a result the ACS is well-defined in electronic terms. A general methodology for locating ACSs for a range of ionic and Menschutkin S_N2 reactions of CH_3X (X = F, Cl, Br, I) derivatives is described. The reactions that were examined span a wide range of reaction energy (over 100 kcal/mol) and possess TSs which spread the gamut from "early" through "late". Nevertheless, all these TSs were found to be located very close to an ACS. Our study indicates that for this wide range of S_N2 reactions there is no simple linkage between TS charge and geometry; TS charge is largely governed by the extent of mixing of the intermediate configuration, while TS geometry is governed by reaction exothermicity. We conclude that the ACS is an excellent approximation for the TS and propose that the ACS may serve as a useful transition-state paradigm in chemical reactivity.

Introduction

Ever since the formulation of transition-state (TS) theory[2] over half a century ago, great effort has been devoted to developing models for characterizing the TS. The reason for this effort is evident; it is the TS that governs the height of the reaction barrier, so any general insight into the nature of the TS is likely to provide greater understanding of those factors that govern chemical reactivity.

Two main approaches to studying the TS have been taken. The first approach, that taken by computational quantum chemistry, has largely sidestepped the inherent problems by adhering to the rigorous mathematical definition of a "saddle point" on a potential energy hypersurface.[3] However, this definition, while of great computational value, provides little practical chemical insight. The formal definition does not, in itself, assist in the organization of experimental data nor does it lead to qualitative predictions about chemical reactivity. In contrast, the second approach, that of the school of physical organic chemistry, has tackled the issue directly through the use of structure-reactivity probes.[4,5] It is true that this approach provides a significantly less rigorous description of the TS; however, it does enable predictions about TS structure and chemical reactivity to be made. The concern is that the absence of a sound theoretical base leaves aspects of the methodology inconclusive, even uncertain.[5] How reliable are the perceived links between empirical structure-reactivity parameters and molecular parameters, and what is the relationship between the quantum chemical and empirical TS pictures? At the present time these questions remain controversial, and a conceptual bridge that connects the two methodologies appears to be lacking. We would hope that a paradigm which offers a fairly rigorous and yet chemically insightful TS description and which is endowed with the capability of making qualitative predictions regarding the nature of the TS may bridge between the methodologies and thereby lead to greater understanding. This paper describes such a potential TS paradigm.

A landmark in the physical organic chemistry methodology of providing a chemically useful description of the TS was achieved by Hammond[6a] and Leffler.[6b] Hammond postulated that two points on a reaction profile that are of similar energy will also be of similar structure. This allowed predictions regarding the structure of the transition state to be made in highly exothermic and endothermic reactions. Leffler generalized the idea to the entire range of reaction exothermicities (although the Leffler relationship is couched in free energy terms) by considering the TS as a hybrid of reactants and products whose character is intermediate between these two extremes. As such, the two approaches have eventually been merged into a single TS paradigm, commonly known as the Leffler-Hammond postulate, which is exemplified in Figure 1a.[4,6c] Thus, as indicated by the arrows on the potential energy profiles, stabilization of the products relative to the reactants is expected to (a) stabilize the TS and (b) shift it to an earlier position along the reaction coordinate, resulting in a TS that is more reactant-like in both its charge distribution and its geometry. The Leffler relationship, written underneath the energy profile in Figure 1a, defines a similarity parameter α which measures the resemblance of the TS to reactant and product on a scale of 0 to unity. The more exoergic the

* Abstract published in *Advance ACS Abstracts*, December 1, 1993.

(1) (a) The former name is Sason S. Shaik. (b) Hebrew University. (c) Address for correspondence: Department of Chemistry, Ben-Gurion University of the Negev, Beer Sheva, Israel 84105. (d) On leave from Ben-Gurion University. (e) Sydney University.

(2) (a) Eyring, H. *J. Chem. Phys.* **1935**, *3*, 107. (b) Wigner, E. *Trans. Faraday Soc.* **1938**, *34*, 29. For summaries, see: (c) Tucker, S. C.; Truhlar, D. G. In *New Theoretical Concepts for Understanding Organic Reactions*; Bertran, J., Csizmadia, I. G., Eds.; NATO ASI Series; Kluwer Academic Publishers: Dordrecht, 1988; Vol. C267, p 291. (d) Hynes, J. T. *Annu. Rev. Phys. Chem.* **1985**, *36*, 573.

(3) For a recent review, see: Schlegel, H. B. *Adv. Chem. Phys.* **1987**, *67*, 249.

(4) For a recent review, see Chapter 1 in the following: Shaik, S. S.; Schlegel, H. B.; Wolfe, S. *Theoretical Aspects of Physical Organic Chemistry. The S_N2 Mechanism*; Wiley: New York, 1992; and references therein.

(5) For an analysis of some of the difficulties with structure-reactivity probes, see: (a) Hoz, S. *Acc. Chem. Res.* **1993**, *26*, 69. (b) Pross, A.; Shaik, S. S. *Nouv. J. Chim.* **1989**, *13*, 427.

(6) (a) Hammond, G. S. *J. Am. Chem. Soc.* **1955**, *77*, 334. (b) Leffler, J. E. *Science* **1953**, *117*, 340. (c) Farcasiu, D. *J. Chem. Educ.* **1975**, *52*, 75.

0002-7863/94/1516-0262$04.50/0

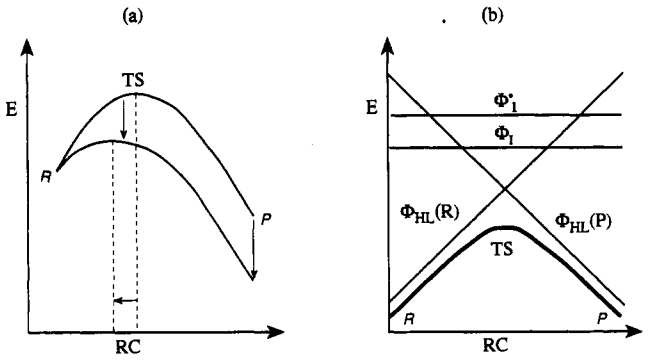

Figure 1. (a) Illustration of the Leffler–Hammond postulate. The arrows show that stabilization of products (P) relative to reactants (R) is expected to shift the TS to (i) lower energy and (ii) an earlier position along the reaction coordinate (RC). The Leffler free energy relationship is shown underneath the reaction profile. (b) Illustration of the avoided crossing paradigm. Reactant and product configurations are indicated by Φ_{HL}(R) and Φ_{HL}(P), respectively, and intermediate VB configurations by Φ_I's. Configuration mixing leads to an avoided crossing, which is shown only for the lowest profile. The final state is shown by the thick line.

reaction, the smaller its similarity parameter α, and the more reactant-like the TS becomes.

The notion of relating the TS to well-defined species has been developed further by the potential energy surface models.[4,7] These consider the variation of the TS, in a perpendicular (or anti-Hammond) direction to the reaction coordinate, not just in a parallel (or Hammond) direction. Thus, while the parallel movement measures the extent of similarity to reactants or products, the perpendicular movement measures the similarity of the TS to potential reaction intermediates.[7a-c] This approach and its quantitative implementation in terms of structrue–reactivity coefficients[7c,8] have evolved into a consistent TS paradigm that views the TS as a species which varies, geometrically and electronically, in a continuous manner among the well-defined structures of reactants, products, and potential intermediates.

Recently, we have proposed an alternative TS paradigm,[8a] based on the curve-crossing model,[8] that builds on the pioneering ideas of Evans.[9] According to this model, the TS is located in the region of *avoided crossing* of the Heitler–London (HL) VB configurations that describe the covalent bonding of reactants and products. Other VB configurations, that describe potential intermediates, mix into the bonding combination of the HL configurations in the avoided crossing region and thereby generate a more complete description of the TS.[8]

Restricting the argument, for the sake of simplicity, to a single intermediate VB configuration, the TS wave function can be expressed approximately by the wave function of an avoided crossing state (ACS), depicted in eq 1, where the term in square brackets is the bonding combination of the HL avoided crossing state function and λ is the mixing coefficient of the intermdiate configuration. A pictorial representation of the mixing procedure

$$\Psi_{TS} \cong \Psi_{ACS} = (1 + \lambda^2)^{-1/2}\{2^{-1/2}[\Phi_{HL}(R) + \Phi_{HL}(P)] + \lambda\Phi_I\} \quad (1)$$

is illustrated in Figure 1b. Thus, the feature that characterizes the ACS is that reactant and product configurations, Φ_{HL}(R) and Φ_{HL}(P), contribute equally to the state wave function. In other words, the ACS is that point on the reaction surface that lies directly beneath the crossing point of Φ_{HL}(R) and Φ_{HL}(P). Inspection of Figure 1b suggests that the ACS and the TS are likely to lie very close to one another on the reaction surface. In fact, it is here that the importance of the ACS concept lies: *the well-defined ACS wave function may serve as an approximate representation for the a priori less well-defined TS wave function.* As such, the mathematically well-defined TS can be complemented with a well-defined quantum mechanical wave function.

Equation 1 refers to the electronic structure, and therefore, provided the approximation in the equation is a good one, it would describe the electronic structure of the TS regardless of its geometry. It follows that, for example in the case of an ionic S_N2 reaction shown in eq 2, the TS will possess approximately equal charges on the nucleophile (Y) and the leaving groups (X) irrespective of the TS geometry. Thus, our TS paradigm implies that the geometry and charge distribution of the TS are not related in the fashion predicted by application of the Leffler–Hammond postulate.[8a]

$$Y:^- + R{-}X \rightarrow Y{-}R + :X^- \quad (2)$$

Recently, Shi and Boyd[10] have carried out an extensive computational study of S_N2 TSs at a high level of theory and have shown, by looking at charge distribution and projected weights of VB structures, that the prediction of charge equality (on X and Y, eq 2) holds for some TSs but not for all and that other factors being equal, a more exothermic reaction leads to a more reactant-like charge distribution. We in turn argued[11] that despite these findings, the entire data set of Shi and Boyd exhibited the effect predicted by the avoided crossing paradigm and that while TS geometries varied with the reaction exothermicity in the fashion predicted by the Leffler–Hammond postulate, the plot of TS charges against exothermicity exhibited a complete scatter.[11] A dependence of TS geometries on exothermicity was pointed out by Wolfe, Mitchell, and Schlegel[12,13] in their early theoretical study of S_N2 reactions. However, no corresponding correlation of the charge development was reported in the Wolfe–Mitchell–Schlegel study.

Recently, Kim and Hynes[14] have also treated the S_N1 reaction theoretically in terms of an avoided crossing model and have found that despite the fact that the location of the TS is very close to the avoided crossing point, the charge distribution still behaves in a manner that would be anticipated from the Leffler–Hammond postulate. Kim and Hynes[14] explained this behavior by showing that the S_N1 avoided crossing interaction varies in an asymmetric fashion on the reactant and product sides of the crossing point, and this variation causes the TS to shift away from the geometry of the crossing point. The effect of this shift on the TS charge distribution results in apparent Leffler–Hammond behavior, i.e., a product-like charge in the TS of the S_N1 bond dissociation.

There are a few other curve-crossing studies[15] which show that the TS is located in the proximity of the crossing point of reactant and product configurations. Since no discussion of the charge distribution patterns accompanies these curve-crossing studies, it is not possible to assess the generality of the Leffler–Hammond behavior regarding TS charges. However, these latter results and those of Kim and Hynes[14] do lead to the following general

(7) (a) Thornton, E. R. *J. Am. Chem. Soc.* **1960**, *82*, 21. (b) More O'Ferrall, R. A. *J. Chem. Soc. B* **1974**, 274. (c) Jencks, W. P. *Chem. Rev.* **1985**, *85*, 511. (d) Harris, J. C.; Kurz, J. L. *J. Am. Chem. Soc.* **1970**, *92*, 349. (e) Critchlow, J. E. *J. Chem. Soc. Faraday Trans. 1* **1972**, *68*, 1774. (f) Albery, W. J. *Prog. React. Kinet.* **1967**, *4*, 355. (g) Grunwald, E. *J. Am. Chem. Soc.* **1985**, *107*, 125.

(8) (a) Pross, A.; Shaik, S. S. *Tetrahedron Lett.* **1982**, *23*, 5467. (b) Pross, A.; Shaik, S. S. *Acc. Chem. Res.* **1983**, *16*, 363. (c) See pages 265–269 in ref 4. (d) Shaik, S. S. *Prog. Phys. Org. Chem.* **1985**, *15*, 197. (e) Pross, A. *Adv. Phys. Org. Chem.* **1985**, *21*, 99.

(9) Evans, M. G.; Warhurst, E. *Trans. Faraday Soc.* **1938**, *34*, 614.

(10) Shi, Z.; Boyd, R. J. *J. Am. Chem. Soc.* **1991**, *113*, 1072.

(11) Pross, A.; Shaik, S. *Croat. Chem. Acta* **1992**, *65*, 625.

(12) Wolfe, S.; Mitchell, D. J.; Schlegel, H. B. *J. Am. Chem. Soc.* **1981**, *103*, 7692.

(13) Mitchell, D. J. Ph.D. Dissertation, Queen's University, Kingston, Canada, 1981.

(14) Kim, H. J.; Hynes, J. T. *J. Am. Chem. Soc.* **1992**, *114*, 10508, 10528.

(15) (a) Sevin, A.; Hiberty, P. C.; Lefour, J. M. *J. Am. Chem. Soc.* **1987**, *109*, 1845. (b) Warshel, A.; Russell, S. *J. Am. Chem. Soc.* **1986**, *108*, 6569. (c) Warshel, A. *Acc. Chem. Res.* **1981**, *14*, 284. (d) Bernardi, F.; Olivucci, M.; Robb, M. A. *Res. Chem. Intermed.* **1989**, *12*, 217.

question: *how good an approximation is the avoided crossing state (ACS) to the TS*? If the ACS wave function is proven to be an effective approximation for the TS wave function, then we have uncovered a simple means of describing the TS, based on the fact that the ACS is relatively well-defined (by eq 1) and therefore possesses a relatively well-defined electronic structure. As mentioned above, there is little common ground to bridge between the quantum mechanical and physical organic schools of thought.[5a,8d] We believe, therefore, that a TS paradigm which manages to merge these two approaches by offering a fairly rigorous and yet chemically meaningful description of the TS would be of value.

We study this question by considering two different classes of S_N2 reactions: the ionic reactions in eq 3 and the Menschutkin[16] reactions in eq 4. These reactions are well-suited for the present

$$Y^- + CH_3X \rightarrow YCH_3 + X^-; \quad X, Y = F, Cl, Br, I \quad (3)$$

$$H_3N + CH_3X \rightarrow H_3N{-}CH_3^+ + X^-; \quad X = F, Cl, Br, I \quad (4)$$

study for several reasons. Firstly, the nucleophiles and leaving groups studied are common in experimental chemistry, so the conclusions of the study will be relevant to widely studied systems. Secondly, the different charge nature of the reactions and the variation of the substituents over four rows of the periodic table provide an extended test for the proposal. Thirdly, the reactions span an enormous range of reaction energy, over 200 kcal/mol, with the ionic reactions being exothermic while the Menschutkin reactions are strongly endothermic (103–150 kcal/mol). So in several important respects this set of reactions is a useful one for testing the avoided crossing paradigm.

There are also some specifically interesting features of the Menschutkin S_N2 reaction which have been studied computationally[17,18] and observed both in the gas phase[19] and in solution.[16,20] In the gas phase the reaction has been interpreted in terms of a covalent–ionic curve crossing and a harpoon-like mechanism[19] (similar to the avoided crossing mechanism used in this paper), but no information was reported on the structure of the TS, other than a general sensitivity of the reaction cross section to steric effects, in accord with expected S_N2 reactivity. In solution, Abraham[21] has used the Menschutkin TS to build up a detailed solvent effect methodology, while the rate–equilibrium studies of Arnett and Reich[22a] and their interpretation have been a source of controversy.[22] The computational results (with and without the inclusion of solvation) by Bertran and his collaborators[17] have been interpreted in terms of the SCD curve-crossing model,[23] and it was noted that while the geometry of the TS was found to vary in the fashion predicted by the Leffler–Hammond postulate, the charge development of the TS was not synchronized to the geometric change but was more advanced because of the coupling of the electronic structure to the solvation. So the Menschutkin reaction is an interesting one in order to test the ACS paradigm, both in the gas phase and in solution.

In this paper we locate both the TSs and ACSs of the target reactions, the former by conventional computational procedures and the latter by procedures described in this paper. It shall be seen that in all the cases studied, as well as for the TSs which were located by Bertran and collaborators,[17] *the ACS is an excellent approximation for the TS*. The implications of this conclusion on TS structure research are discussed.

Methodology and Computational Procedures

The computations were peformed with the GAUSSIAN 90 (REV-J)[24] and GAUSSIAN 92 (REV-C3)[25] series of programs on the IBM-RS/6000 (Model 550) workstations of the Hebrew and Ben-Gurion Universities. The LANL1DZ basis set was used for all structures.[26] This basis set corresponds to a Dunning/Huzinaga valence double-ζ basis (D95V) for first-row elements[27] and to an effective core potential plus double-ζ basis for all higher row elements (Cl, Br, and I).[26] As discussed below, this basis set is deemed suitable for the systems studied in this paper.

The geometries of reactants, products, clusters, and transition states for the target S_N2 reactions, as well as their identity sets, were optimized by gradient methods and checked by frequency calculations using numerical second derivatives (the default option for the above basis set). Optimizations were carried out at the Hartree–Fock (HF) SCF level as well as at the second-order Möller–Plesset level (MP2). Energies were determined at the HF level as well as the MP2(full) and MP4(full) levels, which include the contribution of core electrons to the correlation correction. In all cases frozen core MPn(FC) calculations were used and found to yield virtually the same relative energies, the same geometries, and the same charge distributions as the MPn(full) levels. Shorthand notations are used in the tables and in the text to specify the level of calculation; for example, MP4//MP2 signifies a single-point MP4(full) calculation at the MP2(full)-optimized geometry, while MP2//MP2 signifies a calculation where both energy and geometry were obtained at the MP2(full) level. Frozen core post SCF calculations are specified in parentheses, e.g., MPn(FC)//MPn(FC).

Constructon of an Avoided Crossing State (ACS) Wave Function. Group charges were assigned on the basis of Mulliken population analysis at the HF, MP2, and MP4 levels, where the MP4 charges are correct to second order. The charges were converted to coefficients of the contributing VB structures (see details in the next section). The coefficients served, in turn, to formulate the electronic structure of the TS in terms of the avoided crossing picture. Then, a guess wave function, defined by eq 1 so that it satisifies the avoided crossing constraint, is constructed from the contributing VB configurations, and the closest possible function to the actual TS wave function is determined in each case. This procedure is discussed in detail later in the text (eqs 13–20). It is noted that the Mulliken population analysis is just one of the many methods for obtaining charges,[10,25] and it is entirely possible to couple the procedure to any charge partition scheme.

Location of Avoided Crossing State (ACS) Structures. A geometric search was carried out for each system to locate the ACS structures that are closest to the TSs in both structure and energy. A general procedure for locating such ACSs was established. This procedure involves stepping along the reaction vector (the vibrational mode with the negative eigenvalue in the Hessian) and terminating the procedure at the geometry where the condition for avoided crossing is met. The condition for avoided crossing was tested for by comparing the computed Mulliken group charges at each step with the charge distribution of the ACS guess wave function

(16) Menschutkin, N. *Z. Phys. Chem.* **1890**, *6*, 41.
(17) Sola, M.; Lledos, A.; Duran, M.; Bertran, J.; Abboud, J.-L. *J. Am. Chem. Soc.* **1991**, *113*, 2873.
(18) Gao, J. *J. Am. Chem. Soc.* **1991**, *113*, 7796.
(19) Yen, Y. F.; Cross, R. J.; Saunders, M. *J. Am. Chem. Soc.* **1991**, *113*, 5563.
(20) Okamoto, K.; Fukui, S.; Shingu, H. *Bull. Chem. Soc. Jpn.* **1967**, *40*, 1920, 2354.
(21) (a) Abraham, M. H.; Grellier, P. L. *J. Chem. Soc., Perkin Trans. 2* **1976**, 1735. (b) Abraham, M. H.; Abraham, R. J. *J. Chem. Soc., Perkin Trans. 2* **1975**, 1677. (c) Abraham, M. H. *Pure Appl. Chem.* **1985**, *57*, 1055.
(22) (a) Arnett, E. M.; Reich, R. *J. Am. Chem. Soc.* **1980**, *102*, 5892. (b) Harris, J. M.; Paley, M. S.; Prasthofer, T. W. *J. Am. Chem. Soc.* **1981**, *103*, 5915. (c) Kevill, D. N. *J. Chem. Soc., Chem. Commun.* **1981**, 421.
(23) The SCD is a compact two-curve model and is an alternative to the explicit VB mixing approach in this paper. For the relationship between the SCD and the VBCM curve-crossing models, see ref 4, 8b-e, and the following: (a) Shaik, S. S. *J. Am. Chem. Soc.* **1981**, *103*, 3692. (b) Shaik, S. S.; Pross, A. *J. Am. Chem. Soc.* **1982**, *102*, 2780. (c) Shaik, S. S. *Acta Chem. Scand.* **1990**, *44*, 205.
(24) Frisch, M. J.; Head-Gordon, M.; Trucks, G. W.; Foresman, J. B.; Schlegel, H. B.; Raghavachari, K.; Robb, M.; Binkley, J. S.; Gonzalez, C.; Defrees, D. J.; Fox, D. J.; Whiteside, R. A.; Seeger, R.; Melius, C. F.; Baker, J.; Martin, R. L.; Kahn, L. R.; Stewart, J. J. P.; Topiol, S; Pople, J. A. *Gaussian 90, Revision J*; Gaussian, Inc.: Pittsburgh, PA, 1990.
(25) Frisch, M. J.; Trucks, G. W.; Head-Gordon, M.; Gill, P. M. W.; Wong, M. W.; Foresman, J. B.; Johnson, B. G.; Schlegel, H. B.; Robb, M. A.; Replogle, E. S.; Gomperts, R.; Andres, J. L.; Raghavachari, K.; Binkley, J. S.; Gonzalez, C.; Martin, R. L.; Fox, D. J.; Defrees, D. J.; Baker, J.; Stewart, J. J. P.; Pople, J. A. *Gaussian 92, Revision C3*; Gaussian, Inc., Pittsburgh, PA, 1992.
(26) (a) Hay, J. P.; Wadt, W. R. *J. Chem. Phys.* **1985**, *82*, 270. (b) Wadt, W. R.; Hay, J. P. *J. Chem. Phys.* **1985**, *82*, 284. (c) Hay, J. P.; Wadt, W. R. *J. Chem. Phys.* **1985**, *82*, 299.
(27) Dunning, T. H.; Hay, J. P. *Modern Theoretical Chemistry*; Plenum: New York, 1976; Chapter 1, pp 1–28.

(eqs 15, 16). The charge distribution of the ACS located in this way was then compared with the charge distribution of the best fit guess wave function. In all cases that were examined, the charge distributions by the two procedures were found to be almost identical. Thus, the two procedures for identifying the ACS that is closest to the TS lead to the same result. The geometric search was carried out at the MP2(FC)//MP2(FC) level after verification that the charges, geometries, and relative energies are identical to those at the MP2(full)//MP2(full) level.

To illustrate the procedure for an ACS search, consider the $(Cl\cdots CH_3\cdots Br)^-$ system. The transition-state charges (at the MP2//MP2 level) were found to be $Q(Cl) = -0.66$ and $Q(Br) = -0.56$. The best fit guess ACS wave function, as defined by eq 1 and closest to the TS in its charge distribution, was found to have $Q(Cl) = Q(Br) = -0.61$.

The second procedure for locating the ACS, the geometric search method, was then applied. The reaction vector (RV) for this system is given by eq 5 where all the contributions except for the movements of the heavy atoms are omitted. Accordingly, one steps gradually along this

$$RV = 0.684r_{CBr} - 0.648r_{CCl} + \ldots \quad (5)$$

truncated RV, while optimizing all other geometric parameters. At each step the Mulliken charges are examined, and the search for an ACS is complete once a geometry is found for which the Br and Cl Mulliken charges become equal, irrespective of the individual charges themselves (eq 15). In this specific example, the ACS was found to possess the charges $Q(Cl) = Q(Br) = -0.61$, which are precisely the charges found for the guess ACS wave function with the best fit to the TS. The fact that these two procedures lead to the same result is used as a test of consistency of the two search strategies.

This is a typical search procedure, which for an ionic S_N2 reaction is facilitated because *the ACS is characterized by equal charges on the nucleophile and the leaving group*. In the case of the Menschutkin reactions, one steps along the reaction vector in an analogous manner. However, now the avoided crossing situation is not characterized by charge equality, as in the ionic reactions. Instead, the guess wave function which corresponds to the avoided crossing situation is translated into group charges (eq 16), and at each step along the reaction vector one compares the computed charge distribution against the test charge distribution, until the condition for avoided crossing is reached (eq 16). For example, in the case of the $NH_3\cdots CH_3\cdots Cl$ system, the charges within the geometrically located ACS are $Q(NH_3) = +0.338$, $Q(CH_3) = +0.325$, and $Q(Cl) = -0.664$, in excellent accord with the charges obtained from the guess wave function, $Q(NH_3) = +0.338$, $Q(CH_3) = +0.324$, and $Q(Cl) = -0.662$ using eq 16.

In the case of $NH_3\cdots CH_3\cdots I$ we applied, in addition to the reaction vector methodology, a geometric grid around the transition state to explore the existence of other ACS candidates. The ACS located in this fashion was also found to be close to the TS but less so than the ACS found by the reaction vector methodology (RV). It should be noted that the RV method is an approximate IRC calculation, and ultimately one may wish to explore this latter method as a general procedure for locating ACSs.

Results

A. Reaction Profiles and Relative Energies. Typical computed reaction profiles are presented schematically in Figure 2a,b. Figure 2a shows the well-established double well potential for ionic S_N2 reactions with a barrier flanked by two ion–dipole clusters of the separated reactants and products.[4,10,12,13,28,29] Figure 2b represents the computed reaction profile for the Menschutkin S_N2 reactions. Here the reactant cluster, C_R, is stabilized by dipole–dipole interactions, while the product cluster, C_P, is an ion pair stabilized by strong Coulombic interactions. These general features also appear in the all-electron calculations of Bertran et al.[17] and of Gao.[18]

Tables 1 and 2 list the relative energy data of the critical species for the reaction profiles shown in Figure 2a,b. Inspection of Table 1, with the ionic S_N2 results, reveals several trends. Firstly, with the LANL1DZ basis set, no barrier is found for the reactions with F^-, in line with other calculations of the system F^-/CH_3Cl using split valence basis sets (with and without polarization functions),[4,30] but in disagreement with basis sets that include diffuse functions and which do exhibit a central barrier for this reaction.[31,32] Similarly, our computed barriers for the Cl^-/CH_3Br reaction are smaller in comparison with the corresponding results obtained using Huzinaga's MINI basis set.[33] Indeed, a general feature of the LANL1DZ basis set seems to be its underestimation of the central barriers for ionic reactions, in comparison with more extended basis sets which include diffuse functions. Secondly, the central barriers which are computed for the post-first-row elements are seen to increase upon inclusion of electron correlation in the calculations. This result is in agreement with all electron calculations for Cl^-/CH_3Cl[31,32] and with effective core potential calculations for the same reaction as well as for Br^-/CH_3Br using much more extended basis sets.[34] Thirdly, the reaction thermodynamics are reproduced extremely well in comparison with experiment, especially at the post-SCF levels.

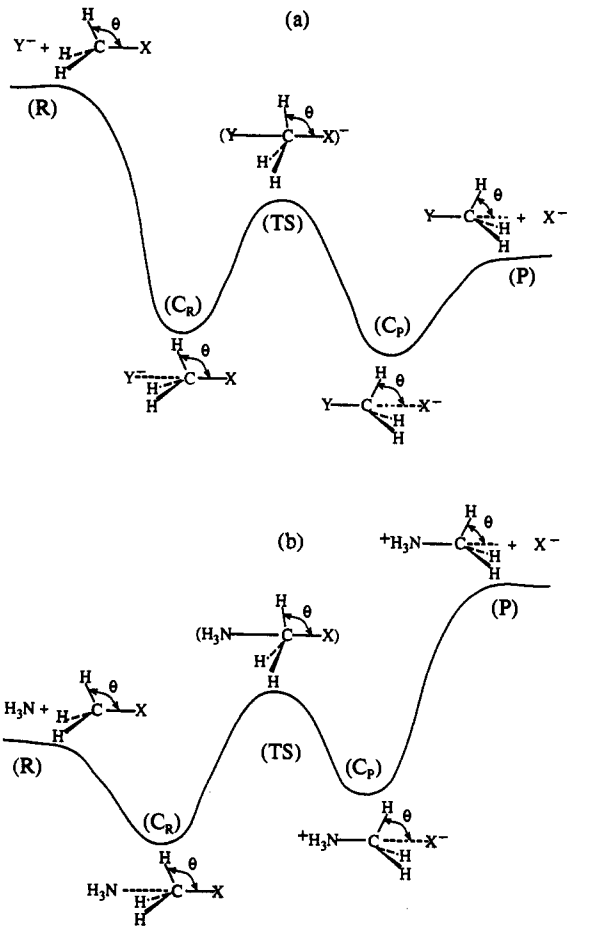

Figure 2. Computed reaction profile types for (a) ionic S_N2 reactions (eq 3) and (b) Menschutkin S_N2 reactions (eq 4).

Table 2 lists the energy data for the Menschutkin reactions, and several trends may be noted. All the reactions are found to be highly endothermic, with the corresponding TSs close in energy to the ion-pair product clusters, C_P. The reaction NH_3/CH_3F does not exhibit a central barrier but proceeds via a reactant cluster smoothly to the products, while all other reactions possess significant barriers. Our central barriers compare favorably with the all-electron HF/3-21G calculations[17] for NH_3/CH_3Br, but are much lower than the MP4//6-31+G* value for NH_3/CH_3Cl.[18] The reaction thermodynamics computed at the post-SCF

(28) Wolfe, S.; Mitchell, D. J.; Schlegel, H. B. *J. Am. Chem. Soc.* **1981**, *103*, 7694.
(29) Pellerite, M. J.; Brauman, J. I. *J. Am. Chem. Soc.* **1980**, *102*, 5993.
(30) See page 89 of ref 13.
(31) Wolfe, S.; Kim, C.-K. *J. Am. Chem. Soc.* **1991**, *113*, 8056.
(32) (a) Shi, Z.; Boyd, R. J. *J. Am. Chem. Soc.* **1989**, *111*, 1575. (b) Shi, Z.; Boyd, R. J. *J. Am. Chem. Soc.* **1990**, *112*, 6789.
(33) Hirao, K.; Kebarle, P. *Can. J. Chem.* **1989**, *67*, 1261.
(34) Vetter, R.; Zulicke, L. *J. Am. Chem. Soc.* **1990**, *112*, 5136.

Table 1. Calculated Relative Energies of the Critical Species[a] in the Ionic S_N2 Reaction, $Y^- + CH_3X \rightarrow YCH_3 + :X^-$

entry[b]	Y, X	R	C_R	TS	C_P	P
1a	Cl, Br	0.0	−14.8	−12.5	−23.2	−10.5
1b			−14.1	−9.6	−20.2	−7.8
1c			−14.6	−11.2	−20.5	−7.7
1d						−7.4
1e						−8.0 (exptl)
2a	Cl, I	0.0	−13.6	−12.5	−28.8	−18.6
2b			−13.0	−9.5	−24.5	−14.8
2c			−13.5	−11.3	−24.9	−15.1
2d						−14.2
2e						−16.0 (exptl)
3a	Br, I	0.0	−10.9	−7.3	−17.7	−8.2
3b			−10.5	−4.8	−15.9	−7.1
3c			−11.0	−6.3	−16.5	−7.4
3d						−6.8
3e						−8.0 (exptl)
4a	Cl, F	0.0				−43.1
4b						−34.3
4c						−34.4
4d						−33.6
4e						−29.0 (exptl)
5a	F, Br	0.0				−53.6
5b						−42.0
5c						−42.1
5d						−40.4
5e						−37.0 (exptl)
6a	F, I	0.0				−61.7
6b						−49.1
6c						−49.5
6d						−46.9
6e						−45.0 (exptl)

[a] In kcal/mol, where R = reactants, C_R = reactant cluster, TS = transition state, C_P = product cluster, P = products. See Figure 2a for structures. [b] For each entry number, the values correspond in the following order to (a) HF//HF, (b) MP2//MP2, (c) MP4//MP2, (d) $\Delta H_{298.15}$ (MP2), (e) experimental values evaluated according to electron affinity and bond energy data in ref 4 (Table 4.3). The basis set is LANL1DZ. Post-SCF options refer to MP*n*(full).

Table 2. Calculated Relative Enegies of the Critical Species[a] in the Menschutkin S_N2 Reaction, $H_3N: + CH_3X \rightarrow H_3NCH_3^+ + :X^-$

entry[b]	X	R	C_R	TS	C_P	P
1a	F	0.0	−2.5			+152.9
1b			−3.3			+152.2
1c			−3.5			+153.0
1d						+153.0
1e						+151.7 (exptl)
2a	Cl	0.0	−2.1	+28.0	+25.1	+109.8
2b			−2.7	+29.2	+28.9	+117.5
2c			−2.9	+29.2	+29.3	+118.6
2d						+121.7
2e						+122.7 (exptl)
3a	Br	0.0	−1.7	+25.1	+20.4	+99.4
3b			−2.3	+27.7	+26.8	+109.7
3c			−2.5	+27.4	+27.3	+111.0
3d						+114.2
3e						+114.7 (exptl)
4a	I	0.0	−1.2	+25.1	+18.4	+91.2
4b			−1.7	+28.6	+26.6	+102.7
4c			−1.9	+27.9	+27.0	+103.6
4d						+107.4
4e						+106.7 (exptl)

[a] In kcal/mol, where R = reactants, C_R = reactant cluster, TS = transition state, C_P = product cluster, P = products. See Figure 2b for structures. [b] For each entry number, the values correspond in the following order to (a) HF//HF, (b) MP2//MP2, (c) MP4//MP2, (d) $\Delta H_{298.15}$ (MP2), (e) experimental values estimated from bond energies and electron affinities in ref 4 (Table 4.3) and the methyl cation affinity of NH_3, taken from Meot-ner, M.; Karpas, Z.; Deakyne, C. A. *J. Am. Chem. Soc.* **1986**, *108*, 3913. The basis set is LANL1DZ. Post-SCF options refer to MP*n*(full).

levels are seen to be in very good agreement with experimental estimates. These and the similar results in Table 1 show that post-SCF calculations with the LANL1DZ basis set give reliable reaction thermodynamics over a range of ~200 kcal/mol. Given that thermodynamics is a key parameter in the application of the Leffler–Hammond postulate, this reliability is important for our analysis.

B. Optimized Geometries. Tables 3 and 4 list the principal geometric parameters of the critical species investigated in this study. Table 3 lists the data for the ionic S_N2 reactions, while Table 4 lists the data for the Menschutkin reactions. Let us focus on the TSs which are of particular interest.

The identity reaction F^-/CH_3F is probably the most theoretically studied S_N2 process. The calculated C–F bond length in the D_{3h} TS ranges between 1.78 and 1.898 Å, depending on the basis set and level of computation.[4,10,12,13,31,32,34,35] Our results of 1.865 Å at the HF-optimized geometry and 1.873 Å at the MP2-optimized geometry are comparable to those obtained with extended basis sets, specifically by Dedieu and Veillard,[35b] Vetter and Zulicke,[34] Duke and Bader,[35c] and Sini et al.[35d] (1.860–1.898 Å), and are slightly longer than the results of Shi and Boyd[32] and Wolfe and Kim[31] (1.836–1.846 Å). The results of split valence basis sets with and without polarization tend to be somewhat shorter (1.78–1.83 Å) than ours.[4,13,35a,f]

The transition state for the Cl^-/CH_3Cl reaction has been studied extensively as well.[4,28,31,32,34,35e,36] The C–Cl bond length in our study, 2.407 Å (HF-optimized geometry) and 2.383 Å (MP2-optimized geometry), is in good agreement with the results of Tucker and Truhlar,[36c] Vetter and Zulicke,[34] Shi and Boyd,[32] and Keil and Ahlrichs,[35e] based on all-electron calculations and an extended basis set (with and without correlation). In fact, in this case the geometry of the transition state is not significantly affected by the basis set, and our results compare well with those obtained with 4-31G,[28] 3-21G*,[36c] and 3-21G basis sets.[36a]

The Br^-/CH_3Br transition state was studied by Vetter and Zulicke[34] using all-electron as well as effective core potential calculations with an extended basis set. Our result for the C–Br bond length (2.59 Å at the HF level and 2.54 Å at the MP2 level) is similar to theirs (2.55 Å; 2.56 Å). The transition state for the I^-/CH_3I reaction cannot be compared with other studies, because to the best of our knowledge ours is the first ab initio investigation of this reaction. We have also studied the identity reaction of $NH_3/CH_3NH_3^+$, and the resulting C–N bond lengths in the transition state (2.099 Å at the HF level and 2.061 Å at the MP2 level) are in good agreement with the calculations of Williams[37] using the 4-31G basis set.

Among the nonidentity reactions in Table 3, only Cl^-/CH_3Br was previously studied, by Kebarle et al.[33] using Huzinaga's MINI basis set, which finds 2.410 and 2.418 Å for the C–Cl and C–Br distances at the transition state. These bond lengths are slightly shorter but comparable to our results.

Table 4 lists the data for the Menschutkin S_N2 reactions. The only other published detailed structural study in the all-electron 3-21G investigation of the reaction NH_3/CH_3Br by Bertran et al.[17] Our HF bond lengths are in good agreement with this study.

C. TS Charge Distribution. Mulliken group charges for the ionic nonidentity reactions are listed in Table 5, while those for the Menschutkin reactions are listed in Table 6. For each entry we report the charges which result from an SCF or a post-SCF wave function at a given optimized geometry, either HF or MP2. Thus, if we compare the first three entries in each table, we can see the effect of electron correlation on the charge distribution

(35) (a) Jaume, J.; Lluch, J. M.; Oliva, A.; Bertran, J. *Chem. Phys. Lett.* **1984**, *106*, 232. (b) Dedieu, A.; Veillard, A. *J. Am. Chem. Soc.* **1972**, *94*, 6730. (c) Bader, R. F. W.; Duke, A. J.; Messer, R. R. *J. Am. Chem. Soc.* **1973**, *95*, 7715. (d) Sini, G.; Shaik, S. S.; Hiberty, P. C. *J. Chem. Soc., Perkin Trans. 2* 1992, 1019. (e) Keil, F.; Ahlrichs, R. *J. Am. Chem. Soc.* **1976**, *98*, 4787. (f) Schlegel, H. B.; Mislow, K.; Bernardi, F.; Bottoni, A. *Theor. Chim. Acta* **1977**, *44*, 245. (g) Baybutt, P. *Mol. Phys.* **1975**, *29*, 389.

(36) (a) Morokuma, K. *J. Am. Chem. Soc.* **1982**, *104*, 3732. (b) Chandrasekhar, J.; Smith, S. F.; Jorgensen, W. L. *J. Am. Chem. Soc.* **1985**, *107*, 154. (c) Tucker, S. C.; Truhlar, D. G. *J. Phys. Chem.* **1989**, *93*, 8138.

(37) Williams, I. H. *J. Am. Chem. Soc.* **1984**, *106*, 7206.

Table 3. Principal Geometric Parameters for the Critical Species of the Ionic S_N2 Reaction, $Y:^- + CH_3X \rightarrow YCH_3 + :X^-$

Y, X	parameter[a]	R[b]	C_R[b]	TS[b]	C_P[b,c]	P[b,c]
F, F	r_{CX}	1.425 (1.475)	1.486 (1.546)	1.865 (1.873)		
	r_{CY}		2.524 (2.469)			
	θ	107.8 (107.4)	106.9 (106.0)	90.0 (90.0)		
	<YCX		180.0 (180.0)	180.0 (180.0)		
Cl, Cl	r_{CX}	1.859 (1.880)	1.938 (1.940)	2.407 (2.383)		
	r_{CY}		3.099 (3.077)			
	θ	107.2 (107.6)	105.7 (106.9)	90.0 (90.0)		
	<YCX		180.0 (180.0)	180.0 (180.0)		
Br, Br	r_{CX}	2.013 (2.029)	2.085 (2.080)	2.585 (2.544)		
	r_{CY}		3.339 (3.286)			
	θ	107.1 (107.7)	105.7 (107.1)	90.0 (90.0)		
	<YCX		180.0 (180.0)	180.0 (180.0)		
I, I	r_{CX}	2.181 (2.194)	2.236 (2.230)	2.788 (2.739)		
	r_{CY}		3.692 (3.623)			
	θ	107.4 (108.2)	106.4 (107.9)	90.0 (90.0)		
	<YCX		180.0 (180.0)	180.0 (180.0)		
Cl, Br	r_{CX}	2.013 (2.029)	2.110 (2.092)	2.450 (2.469)	3.360 (3.292)	1.859 (1.880)
	r_{CY}		3.063 (3.063)	2.547 (2.460)	1.921 (1.931)	
	θ	107.1 (107.7)	105.1 (106.9)	94.0 (92.7)	73.9 (73.0)	72.8 (72.4)
	<YCX		180.0 (180.0)	180.0 (180.0)	180.0 (180.0)	
Cl, I	r_{CX}	2.181 (2.194)	2.289 (2.257)	2.547 (2.607)	3.702 (3.626)	1.859 (1.880)
	r_{CY}		3.051 (3.071)	2.655 (2.518)	1.907 (1.918)	
	θ	107.4 (108.2)	105.8 (107.4)	96.9 (94.7)	73.6 (72.7)	72.8 (72.4)
	<YCX		180.0 (180.0)	180.0 (180.0)	180.0 (180.0)	
Br, I	r_{CX}	2.181 (2.194)	2.258 (2.245)	2.678 (2.678)	3.689 (3.623)	2.013 (2.029)
	r_{CY}		3.337 (3.281)	2.694 (2.605)	2.066 (2.066)	
	θ	107.4 (108.2)	105.9 (107.6)	93.1 (92.2)	73.8 (72.6)	72.9 (72.3)
	<YCX		180.0 (180.0)	179.9 (180.0)	180.0 (180.0)	

[a] The parameters refer to the structures in Figure 2a. Distances in angstroms and angles in degrees. [b] Values in parentheses correspond to MP2-optimized geometries. Other values correspond to HF-optimized geometries. The basis set is LANL1DZ. The post-SCF results correspond to MP*n*(full). [c] For the identity reactions (first four entries) data for C_P and P are the same as for C_R and R by symmetry.

Table 4. Principal Geometric Parameters for the Critical Species of the Menschutkin S_N2 Reaction, $H_3N: + CH_3X \rightarrow H_3NCH_3^+ + :X^-$

X	parameter[a]	R[b]	C_R[b]	TS[b]	C_P[b]	P[b]
Cl	r_{CX}	1.859 (1.880)	1.868 (1.888)	2.529 (2.583)	2.837 (2.735)	∞
	r_{NC}	∞	3.469 (3.308)	1.871 (1.784)	1.589 (1.627)	1.528 (1.556)
	θ	107.2 (107.6)	107.2 (107.8)	82.1 (78.9)	72.0 (74.2)	71.7 (72.0)
	<NCX		179.9 (180.0)	180.0 (180.0)	180.0 (180.0)	
	r_{CH}	1.075 (1.096)	1.073 (1.094)	1.066 (1.088)	1.072 (1.091)	1.077 (1.097)
	r_{NH}	0.994 (1.016)	0.997 (1.019)	1.005 (1.029)	1.007 (1.030)	1.010 (1.034)
	<HNC		103.7 (105.3)	108.9 (109.3)	110.0 (109.8)	110.8 (110.7)
Br	r_{CX}	2.013 (2.029)	2.021 (2.034)	2.674 (2.710)	3.048 (2.933)	
	r_{NC}	∞	3.548 (3.356)	1.920 (1.826)	1.578 (1.638)	
	θ	107.1 (107.7)	107.2 (108.0)	83.3 (80.1)	72.2 (73.5)	
	<NCX		180.0 (179.9)	180.0 (180.0)	180.0 (180.0)	
	r_{CH}	1.075 (1.097)	1.073 (1.095)	1.067 (1.088)	1.073 (1.092)	
	r_{NH}	0.994 (1.016)	0.997 (1.018)	1.005 (1.028)	1.007 (1.030)	
	<HNC		103.4 (105.1)	108.7 (109.0)	110.1 (109.9)	
I	r_{CX}	2.181 (2.194)	2.187 (2.186)	2.862 (2.893)	3.308 (3.194)	
	r_{NC}	∞	3.707 (3.476)	1.959 (1.864)	1.569 (1.620)	
	θ	107.4 (108.2)	107.5 (108.5)	84.2 (81.0)	72.0 (72.2)	
	<NCX		183.3 (180.0)	180.0 (180.0)	180.0 (180.1)	
	r_{CH}	1.075 (1.097)	1.070 (1.096)	1.067 (1.088)	1.073 (1.093)	
	r_{NH}	0.994 (1.016)	0.996 (1.018)	1.004 (1.028)	1.008 (1.031)	
	<HNC		108.5 (108.0)	110.0 (109.8)	110.1 (110.0)	

[a] The parameters refer to the structures in Figure 2b. Distances in angstroms and angles in degrees. [b] In each entry, the value in parentheses correspond to MP2-optimized geometries. The other values correspond to HF-optimized geometries. The basis set used is LANL1DZ. The post-SCF results correspond to MP_n(full). For the $H_3N\cdots CH_3F$ C_R cluster the parameters in respective order are the following: 1.431 (1.482); 3.336 (3.191); 107.9 (107.5); 180.0 (180.0); 1.077 (1.096); 0.997 (1.019); 103.8 (105.7).

at a fixed geometry. If, however, we compare entry 1 with 4, 2 with 5, and 3 with 6, we can see how the charge distribution is affected by a change of geometry.

Inspection of entries 1–3 in Table 5 reveals that electron correlation reduces the absolute magnitude of the charges relative to the SCF level, and the same applies to entries 1–3 of Table 6. This effect of electron correlation on charge distribution is expected and has been noted by Hiberty and collaborators[38a-e] as well as by Malrieu and collaborators.[38f,g] If we compare entry 1 with 4, 2 with 5, and 3 with 6, we again encounter the same trend in both Tables 5 and 6, namely, that as the geometry of the TS varies from HF to MP2, electronic charge flows from the nucleophile to the leaving group, while the charge on the central CH_3 group remains essentially constant. If we combine this information with the geometric changes in Tables 3 and 4, we can see that, in comparison with the HF geometry of the TS, the MP2 geometry involves a shorter bond between the nucleophile and the central methyl and a longer bond between the central methyl and the leaving group. Thus, the charge flow is seen to be coupled

(38) (a) Hiberty, P. C.; Leforestier, C. *J. Am. Chem. Soc.* **1978**, *100*, 2012. (b) Hiberty, P. C.; Cooper, D. L. *J. Mol. Struct. (THEOCHEM)* **1988**, *169*, 437. (c) Hiberty, P. C. *Isr. J. Chem.* **1983**, *23*, 10. (d) Hiberty, P. C. *Int. J. Quantum Chem.* **1981**, *XIX*, 259. (e) Hiberty, P. C.; Ohanessian, G. *J. Am. Chem. Soc.* **1982**, *104*, 66. (f) Karafiloglu, P.; Malrieu, J.-P. *Chem. Phys.* **1986**, *104*, 383. (g) LePetit, M.-B.; Ouija, B.; Malrieu, J.-P.; Maynau, D. *Phys. Rev. A.* **1989**, *39*, 3274.

Table 5. Transition-State Charge Distributions in the Anionic S_N2 Transition States, $(Y\cdots CH_3\cdots X)^-$

		$(Cl\cdots CH_3\cdots Br)^-$ [c]			$(Br\cdots CH_3\cdots I)^-$ [c]			$(Cl\cdots CH_3\cdots I)^-$ [c]		
geometry[a]	wave function[b]	Q(Cl)	$Q(CH_3)$	Q(Br)	Q(Br)	$Q(CH_3)$	Q(I)	Q(Cl)	$Q(CH_3)$	Q(I)
1 HF	HF	−0.763	0.364	−0.601	−0.726	0.312	−0.587	−0.795	0.289	−0.494
2 HF	MP2	−0.697	0.218	−0.521	−0.655	0.162	−0.507	−0.736	0.151	−0.416
3 HF	MP4	−0.712	0.244	−0.532	−0.670	0.189	−0.519	−0.750	0.175	−0.426
4 MP2	HF	−0.729	0.362	−0.632	−0.690	0.303	−0.613	−0.741	0.310	−0.569
5 MP2	MP2	−0.660	0.215	−0.560	−0.617	0.156	−0.538	−0.670	0.165	−0.495
6 MP2	MP4	−0.673	0.241	−0.570	−0.631	0.181	−0.550	−0.685	0.190	−0.505

[a] Geometry optimization level using the LANL1DZ basis set. [b] The level at which charge distribution is determined. [c] Mulliken group charges.

Table 6. Transition-State Charge Distributions in the Menschutkin S_N2 Transition States, $H_3N\cdots CH_3\cdots X$

		X = I[c]			X = Br[c]			X = Cl[c]		
geometry[a]	wave function[b]	$Q(NH_3)$	$Q(CH_3)$	Q(I)	$Q(NH_3)$	$Q(CH_3)$	Q(Br)	$Q(NH_3)$	$Q(CH_3)$	Q(Cl)
1 HF	HF	0.221	0.413	−0.634	0.230	0.442	−0.672	0.247	0.464	−0.711
2 HF	MP2	0.270	0.263	−0.533	0.280	0.301	−0.581	0.298	0.328	−0.626
3 HF	MP4	0.258	0.300	−0.559	0.268	0.336	−0.604	0.286	0.361	−0.647
4 MP2	HF	0.280	0.413	−0.693	0.291	0.431	−0.722	0.307	0.448	−0.756
5 MP2	MP2	0.333	0.276	−0.609	0.342	0.304	−0.647	0.359	0.325	−0.684
6 MP2	MP4	0.321	0.312	−0.632	0.330	0.336	−0.666	0.347	0.356	−0.702

[a] Geometry optimization level using the LANL1DZ basis set. [b] The level at which charge distribution is determined. [c] Mulliken group charges.

to the change in geometry. This finding is significant and will be helpful in the three-dimensional search for the ACS from the TS.

How reliable is the charge distribution produced by the LANL1DZ basis set? One assessment of reliability (within the confines of the observability criterion of charge distribution) is by comparison with other computations at the all-electron level. The nonidentity reactions which have been computed by others are Cl^-/CH_3Br,[33] NH_3/CH_3Br,[17] and NH_3/CH_3Cl.[18] In these three cases there is a reasonable match between the LANL1DZ charges in Tables 5 and 6 and the reported charges with the other basis sets. In the case of the identity reactions (not shown in the tables) the charge distributions are generally smaller than, but in reasonable agreement with, all-electron calculations involving extended basis sets, as well as more sophisticated charge partition schemes. Thus, the $F\cdots CH_3\cdots F^-$ TS in our study possesses a post-SCF charge on F of −(0.692–0.703) in comparison with −0.71 in VB calculations with the 6-31G basis set[39] and with a Bader charge of −0.76 at the MP2/6-31++G** level.[10] Similarly, in the $Cl\cdots CH_3\cdots Cl^-$ TS our post-SCF charges are −(0.621–0.648) in comparison with charges of −(0.70–0.72) at levels such as MP2/6-31+G*, MP2/6-31G**,[36c] and MP2/6-31++G**/Bader-partition.[10]

In summary, post-SCF calculations with the LANL1DZ basis set have some deficiencies, notably the underestimation of central barriers. However, this computatioal level reproduces the reaction thermodynamics extremely well, produces reliable TS geometries and reasonable charges, and does so consistently for all the target reactions involving atoms from four different rows of the periodic table. We feel therefore that the choice of the basis set and the level of calculation are suited to the problem we wish to investigate.

Discussion

A. The Electronic Structure of the TS. The idea of describing the TS, a position on the reaction surface that is not well-defined in chemical terms, by another point that is relatively well-defined—the ACS—opens up new avenues for analyzing the TS. The procedure involves describing the ACS (and hence the TS) in terms of contributing effective[40] VB configurations. This approach has been previously applied by us[4,8d] and by Shi and Boyd[10] and forms the basis for the TS paradigm. However, the point we now need to establish is *how valid is the use of the ACS as an approximate representation of the TS*? Let us commence the analysis by considering the VB configurations from which the ACS and TS are constructed.

The important VB configurations which contribute to the S_N2 TS are shown in **1a–3a** for the ionic S_N2 reactions and in **1b–3b** for the Menschutkin S_N2 reactions. In each case there are two Heitler–London (HL) configurations; one (Φ_1) describes the spin-pair bonding between the central carbon to the leaving group (X), and the other (Φ_2) describes the same bonding between the central carbon and the nucleophile (Y or NH_3). The third configuration (Φ_3) is the carbonium ion structure, a triple ion, **3a**, in the ionic cases and an ion pair, **3b**, in the Menschutkin cases.

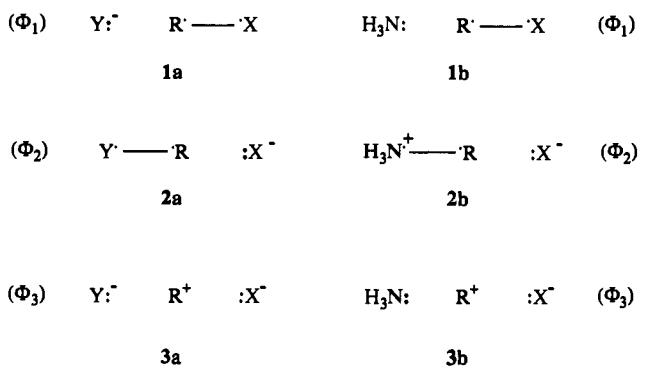

There are also carbanionic configurations, which are exemplified in **4–6**, for the ionic S_N2 reactions. Usually it is assumed that these configurations are high in energy in the vicinity of the TS and would not therefore contribute significantly to its electronic structure.[8,10,11] If the carbanion configurations are indeed negligible, then the conversion of group charges into coefficients of the VB configurations **1–3** becomes straightforward (eqs 7–12).

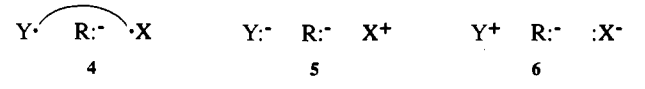

Can the carbanion configuration be safely ignored? Previous experience with VB analyses of MO and MO–CI correlated wave functions, using the Hiberty–Leforestier VB projection technique[38a] as well as by direct VB computations,[39] shows that the assumption that **4–6** are unimportant is justified for S_N2 and analogous TS species. For example, the weight of **4** in the $F\cdots CH_3\cdots F^-$ TS is

(39) Sini, G.; Hiberty, P. C.; Shaik, S. Unpublished data related to ref 35d.
(40) Shaik, S. S. In *New Theoretical Concepts for Understanding Organic Reactions*, Bertran, J., Csizmadia, I. G., Eds.; NATO ASI Series; Kluwer Academic Publishers: Dordrecht, 1988; Vol. C267, p 165.

Table 7. Coefficients of VB Configurations for the Transition States $(Y\cdots CH_3\cdots X)^-$ of the Ionic S_N2 Reactions

		Y, X = Cl, Br[c]			Y, X = Cl, I[c]			Y, X = Br, I[c]		
geometry[a]	wave function[b]	a_1	a_2	a_3	a_1	a_2	a_3	a_1	a_2	a_3
1 HF	HF	0.632	0.487	0.603	0.711	0.453	0.538	0.688	0.523	0.503
2 HF	MP2	0.692	0.550	0.467	0.702	0.587	0.402	0.765	0.515	0.389
3 HF	MP4	0.684	0.537	0.494	0.694	0.574	0.435	0.758	0.501	0.418
4 MP2	HF	0.606	0.520	0.602	0.622	0.557	0.550	0.657	0.509	0.557
5 MP2	MP2	0.666	0.585	0.464	0.711	0.574	0.406	0.679	0.619	0.395
6 MP2	MP4	0.657	0.572	0.492	0.704	0.561	0.436	0.671	0.607	0.425

[a] Geometry optimization level using the LANL1DZ basis set. [b] The level at which charge distribution is determined. [c] The coefficients a_i (i = 1, 2, 3) refer to the configuration Φ_i (i = 1, 2, 3) in **1–3**.

Table 8. Coefficients of VB Configurations for the Transition States $(H_3N\cdots CH_3\cdots X)$ of the Menschutkin S_N2 Reactions

		X = Cl[d]			X = Br[d]			X = I[d]		
geometry[a]	wave function[b]	a_1	a_2	a_3	a_1	a_2	a_3	a_1	a_2	a_3
1 HF	HF	0.538	0.497	0.681	0.573	0.480	0.665	0.605	0.470	0.643
2 HF	MP2	0.612	0.546	0.573	0.647	0.529	0.557	0.683	0.520	0.513
3 HF	MP4	0.594	0.535	0.601	0.629	0.518	0.580	0.664	0.508	0.548
4 MP2	HF	0.494	0.554	0.669	0.530	0.540	0.657	0.550	0.530	0.640
5 MP2	MP2	0.562	0.599	0.570	0.594	0.586	0.551	0.625	0.577	0.525
6 MP2	MP4	0.546	0.589	0.597	0.578	0.574	0.580	0.607	0.567	0.559
7 HF	HF/3-21G,[c] ϵ = 1				0.525	0.518	0.678			
8 HF	HF/3-21G,[c] ϵ = 78.3				0.640	0.390	0.660			

[a] Geometry optimization level using the LANL1DZ basis set. [b] The level at which charge distribution is determined. [c] Results from ref 17. ϵ refers to the dielectric constant. ϵ = 1 is in the gas phase. [d] The coefficients a_i (i = 1, 2, 3) refer to the configuration Φ_i (i = 1, 2, 3) in **1–3**.

only 2.6%, while those of **5** and **6** are less than 0.1%.[39] Even in the $H\cdots CH_3\cdots H^-$ TS, the weight of **4** is 1%, while the weights of **5** and **6** are 0.08%.[39] Similarly, in $F\cdots H\cdots F^-$ the weight of the hydrido configuration, type **4**, is 1.8%, while the other hydrido configurations have virtually zero weights.[39] Furthermore, in all these cases the weight of configuration **3** or of its analog in FHF^- is very close to the charge on the central group. We believe that we are therefore justified in proceeding with our VB analysis, based on configurations Φ_1–Φ_3 in **1–3**.[41]

Following the above discussion, the electronic state wave function of the TS can be expressed as a normalized linear combination of the three contributing VB structures Φ_1–Φ_3 (**1a–3a** in the case of the ionic S_N2 TS, **1b–3b** in the case of the Menschutkin S_N2 TS) as shown in eq 6. The mixing coefficients

$$\Psi_{TS} = \sum_i a_i \Phi_i; \quad i = 1\text{–}3 \tag{6}$$

a_i can be obtained from the absolute magnitudes of the group charges, using eqs 7–9 for the ionic cases,

$$a_1 = [|Q(Y)| - |Q(R)|]^{1/2} \tag{7}$$

$$a_2 = [|Q(X)| - |Q(R)|]^{1/2} \tag{8}$$

$$a_3 = [|Q(R)|]^{1/2} \tag{9}$$

and eqs 10–12 for the Menschutkin cases,

$$a_1 = [1 - |Q(X)|]^{1/2} \tag{10}$$

$$a_2 = [|Q(NH_3)|]^{1/2} \tag{11}$$

$$a_3 = [|Q(R)|]^{1/2} \tag{12}$$

Tables 7 and 8 list the VB coefficients at the various computational levels, and a few common features may be noted. First, it is seen that the wave functions at the MP2 and MP4 levels are similar and that electronic correlation increases the coefficients of the HL configurations at the expense of the coefficient of the carbocation configuration, a_3. A second common feature to the two reaction types can be revealed by inspecting how the weights of the configurations change when the TS geometry varies at the same computational level. Thus, comparisons of entries 1 vs 4, 2 vs 5, and 3 vs 6 in each table show that the coefficient a_3 remains constant for such a structural change, while the product configuration becomes more important at the expense of the reactant configuration (a_2 increases; a_1 decreases). These changes in the coefficients, a_1 and a_2, reflect the strengthening of the bonding between the nucleophile (Nuc) and the central carbon and the simultaneous weakening of the bonding to the leaving group (LG), as the geometry changes in the direction depicted in **7**. Furthermore, these bonding changes

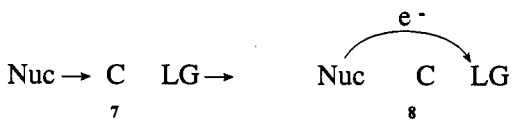

7 8

are accompanied by a charge flow in the direction indicated in **8**. It appears therefore that there is some synchronicity in the charge development, the geometry progression, and the bonding development, and as is discussed subsequently, this kind of synchronicity is expected in the region of the avoided crossing of the HL structures.

Let us now explore the validity of the TS paradigm and investigate whether the TS may be usefully approximated by an ACS. This is carried out for each of the two reaction types by focusing on a computational level in which both the geometry, and the wave function are treated at the same level, namely, the MP2//MP2 level. Table 9 summarized the essential features of the ionic TSs at this level. Shown are the weights of the three configurations a_1-a_3, the percentages of bond breaking[42] in the TS relative to reactant and product bonds, and the bond orders of the TS. The latter quantities are calculated using the method of Wolfe et al.[12] that assigns a total bond order of unity to the corresponding identity TSs.

Inspection of the weights of the HL configurations for the ionic reactions (Table 9) shows that $a_1 > a_2$; that is, the TS wave

(41) An anlogous conclusion has been reached by Wofle and Kim[31] with regard to the importance of the Φ_1–Φ_3 configurations based on the calculated isotope effects.

(42) For a discussion of these percentages of bond cleavage and their correlation with barriers, see: (a) Reference 4, Chapter 6. (b) Shaik, S. S.; Schlegel, H. B.; Wolfe, S. *J. Chem. Soc., Chem. Commun.* **1988**, 1322.

Table 9. Some Properties of $(Y\cdots CH_3\cdots X)^-$ Transition States[a]

	$Br\cdots CH_3\cdots I^-$	$Cl\cdots CH_3\cdots Br^-$	$Cl\cdots CH_3\cdots I^-$
a_1[b]	0.68	0.67	0.71
a_2[b]	0.62	0.59	0.57
a_3[b]	0.40	0.46	0.41
% $CX^{\ddagger}$[c]	19.3	18.2	15.5
% $CY^{\ddagger}$[c]	26.1	27.4	31.3
$n_{CX^{\ddagger}}$[d]	0.540	0.553	0.591
$n_{CY^{\ddagger}}$[d]	0.461	0.450	0.415
$\Delta E_{R,P}$[e]	-7.1	-7.8	-14.8
$\Delta E_{C_R,C_P}$[e]	-5.4	-6.1	-11.5

[a] The properties correspond to the consistent MP2//MP2 level. [b] These are rounded-off figures of the VB coefficients from Table 7. [c] Percentage of bond cleavage defined as % $CL^{\ddagger} = 100[(r_{CL^{\ddagger}} - r_{CL}^0)/r_{CL}^0]$; L = X, Y. [d] Bond orders defined as $n_{CL^{\ddagger}} = \exp[-(r_{CL^{\ddagger}} - r_{CL}^0)/a_{CL}]$; L = X, Y. $a_{C,Cl}$ = 0.726 Å; $a_{C,Br}$ = 0.743 Å; $a_{C,I}$ = 0.786 Å. The a_{CL} (the Pauling constants) values are determined as described in refs 12 and 13 and in Chapter 6 in ref 4, by setting the bond orders at all the indentity reactions at 0.5. [e] Reaction energies from R to P and from cluster C_R to cluster C_P in kcal/mol.

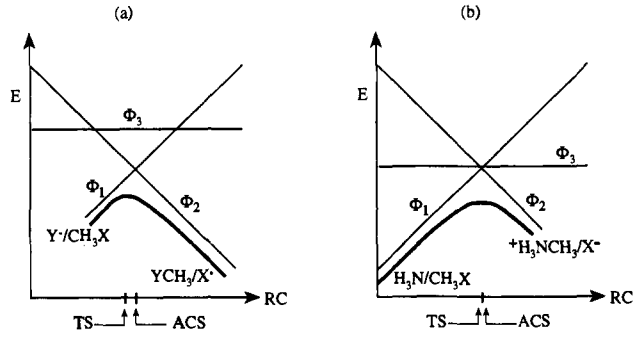

Figure 3. Avoided crossing situations for the ab initio computed TSs based on analysis of the VB coefficients of Φ_1–Φ_3 (**1**–**3**) in (a) ionic S_N2 reactions and (b) Menschutkin S_N2 reactions. In a, the TS is shifted relative to the ACS (located beneath the crossing point of the HL structures (Φ_1, Φ_2). In b, the TS and the ACS almost coincide. Note, also, that the three configurations are all almost degenerate at the crossing point.

function possesses an excess of reactant character. The coefficient, a_3, of the triple ion carbocation structure is seen to be larger for the TS which involves Cl and Br and smallest for the TS which involves Br and I. Indeed, on the basis of the same trend, obtained from analysis of the identity reactions, we may conclude that the importance of the triple ion structure increases with the electronegativities of the nucleophile and the leaving group.

These two pieces of information being combined, the wave function of the TS can be assigned to the avoided crossing situation depicted in Figure 3a, where it appears that *the avoided crossing interaction shifts the TS location to a somewhat earlier position (labeled TS) relative to the crossing point of the HL configurations (labeled ACS)*. If the TS were at the crossing point of reactant and product configurations, than we would find that $a_1 = a_2$. Since $a_1 > a_2$, we must conclude that the TS is located at a geometry where the reactant configuration is *lower* in energy (and hence contributes more to the wave function) than the product configuration.

The asymmetry of the avoided crossing interaction may be caused by the same effect that was discussed by Kim and Hynes[14] for the location of the S_N1 TS, namely, the mixing of $C^+:X^-$ into the HL configuration, which will be larger at short C–X distances.[43] Thus, in the $Cl\cdots CH_3\cdots X^-$ (X = Br, I) TS, this means that on the left-hand side of the crossing point in Figure 3a, where the C–Cl bond is longer, the mixing will be smaller than on the right-hand side of the crossing point, where the C–Cl bond is shorter.[43] Alternatively, it is possible that curve-skewing effects[8,11] may contribute to the earlier location of the TS relative to the crossing point. Whatever the reason, we can conclude therefore that in the ionic S_N2 reactions the TS and ACS are somewhat apart. However, as shall be demonstrated in the following section, the TSs and the ACSs are still very close to one another, so that *the above effects merely shift the TS within the avoided crossing region.*

(43) Since the $C^+:Y^-$ mixing into C–Y becomes larger as Y becomes more electronegative, it follows that for $(Y\cdots C\cdots X)^-$, the triple ion configuration, Φ_3, will mix more heavily into the HL structures in the regions of shorter distances between C and the *more* electronegative ligand (X or Y). In the present case therefore mixing is dominated by the C–Cl bond rather than the C–Br or C–I bonds and is likely to create the effect observed by Kim and Hynes.[14]

Table 10. Some Properties of $(NH_3\cdots CH_3\cdots X)$ Transition States

	I[a]	Br[a]	Cl[a]	Br[b]
a_1[c]	0.63	0.59	0.56	0.52 (0.64)
a_2[c]	0.58	0.59	0.60	0.53 (0.30)
a_3[c]	0.53	0.55	0.57	0.68 (0.66)
% $CX^{\ddagger}$[d]	31.9 (15.1)	33.6 (7.6)	37.4 (5.6)	30.3 (24.0)
% $CN^{\ddagger}$[d]	19.8 (9.4)	17.4 (11.5)	14.6 (7.7)	21.5 (32.2)
$n_{CX^{\ddagger}}$[e]	0.41	0.40	0.38	0.44 (0.62)
$n_{CN^{\ddagger}}$[e]	0.68	0.71	0.75	0.65 (0.43)
$\Delta E_{R,P}$[f]	102.7	109.9	117.5	103.8 (–)
$\Delta E_{C_R,C_P}$[f]	26.6	26.8	28.9	20.7 (-27.2)

[a] Properties obtained at the MP2//MP2 level. [b] Values correspond to the results of Bertran et al. (ref 17). Values in parentheses correspond to a solvent with ϵ = 78.3. [c] These are rounded-off figures of VB coefficients from Table 8. [d] Percentage of bond cleavage as defined in footnote c of Table 9. Values in parentheses correspond to percentages of bond cleavage relative to the geometry of the ion-pair product cluster. [e] Bond orders as defined in footnote d of Table 9. [f] Reaction energies from reactant to product (R, P) and from cluster to cluster (C_R, C_P) in kcal/mol.

The geometry indexes in Table 9 are in agreement with the preceding conclusion and show that the ionic TSs are characterized by a smaller degree of C–X bond breaking relative to Y–C bond making. A similar picture is provided by the Wolfe–Mitchell–Schlegel bond orders[12] in the table. These in turn correlate with the exothermicity of the reactions, as has been pointed out by Shi and Boyd in their study of other ionic reactions.[10]

Let us turn now to Table 10 to inspect the Menschutkin TSs. Here we see in all cases that the carbocation configuration is virtually as important as the two HL configurations. The importance of the carbocation configuration is not confined to just the TS region. In fact, the $C-N^+$ bond in the $CH_3-NH_3^+$ product is described by a wave function with a 0.61 coefficient of the carbocation configuration, $CH_3^+:NH_3$. This reflects the special nature of the $C-N^+$ bond as a charge-shift resonating bond, which acquires a substantial fraction of its bonding from the resonance mixing of the HL configuration ($C^{\cdot}\text{-}N^{+}$) and the carbocation configuration ($C^+:N$).[44,45] *However, of special significance is the fact that a_1 and a_2 values are close in magnitude; that is, the Menschutkin TSs all lie in the proximity of the crossing point of the HL structures* and therefore correspond to the avoided crossing situation depicted in Figure 3b, where the TS and ACS are seen to lie in close proximity. Clearly, Menschutkin TSs do not exhibit any so-called Leffler–Hammond behavior with respect to TS charge; all the reactions are extremely endothermic, yet the electronic structure contains similar contributions of reactant and product configurations.

The geometric features of the Menschutkin TSs are also of interest. From the percentages of bond cleavage[4,42] it is apparent that geometrically the TSs resemble the ion-pair product cluster, and as such are geometrically "late", in accord with the Leffler–Hammond effect that is expected from the large endothermicities of those reactions. From the bond order information it is apparent that, in addition to their being "late", these TSs are also "tight", having a total bond order of more than unity. Thus, in the

(44) (a) Shaik, S. S. In *Molecules in Natural Science and Medicine*; Maksic, Z. B.; Maksic, M.-E., Eds.; Ellis Horwood: London, 1991. (b) Goldstein, S.; Czapski, G.; Cohen, D.; Meyerstein, D.; Shaik, S.; Cho, J. K. *Inorg. Chem.* **1992**, *31*, 798.

(45) Shaik, S.; Maitre, P.; Sini, G.; Hiberty, P. C. *J. Am. Chem. Soc.* **1992**, *114*, 7861.

Menschutkin TSs the variations in electronic structure and geometry are *not* synchronous; the electronic charge is governed by the configurational mix in the TS region, while the geometry is governed by the position of crossing of reactant and product configurations.

This feature of the Menschutkin reaction has been discussed by Bertran et al.,[17] who concluced that upon changing the environment from gas phase to aqueous solution ($\epsilon = 78.3$), the structure becomes geometrically earlier, but the electronic structure does not vary in a synchronous fashion with the geometry. The results of Bertran et al.[17] are shown in the last column of Table 10. It is seen that in the gas phase the TS lies virtually at the crossing point of the HL structures ($a_1 = 0.52$; $a_2 = 0.53$) and possesses a large ion-pair contribution ($a_3 = 0.68$). In aqueous solution ($\epsilon = 78.3$) however, where the ion-pair configuration is now strongly stabilized, the TS moves to an earlier position geometrically, but as may be seen from the VB coefficients in the table, *this TS now comes about from a different avoided crossing, one between the reactant configuration, Φ_1, and the ion-pair carbocation configuration, Φ_3.* This is apparent from the coefficients, a_1 and a_3, that are now very close in magnitude ($a_1 = 0.64$; $a_3 = 0.66$). Thus, in the case studied by the Bertran group, the avoided crossing situation in solution phase resembles an S_N1 avoided crossing, as is illustrated schematically in **9**.

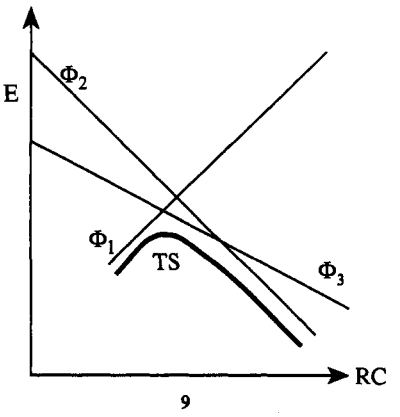

9

B. How Far are the Transition States from Avoided Crossing States? At this point we wish to unify the preceding TS pictures of the two reaction types, by answering the title question in two independent ways. Firstly, we seek an answer in terms of electronic structure, namely, how "far" is the wave function of the computed TS from the wave function of an avoided crossing state (ACS)? Secondly, we seek an answer in structural and energetic terms: how "far" are the structure and energy of the computed TS from those of an ACS? If both answers suggest that the TS and ACS are close to one another, structurally and electronically, then *we have provided a strong basis for our proposal that an ACS may serve as a useful approximation for a TS.*

Wave Function for Avoided Crossing States. The avoided crossing wave function of the two HL structures, the HL state, is given by a linear combination of Φ_1 and Φ_2.

$$\Phi_{HL} = 2^{-1/2}[\Phi_1 + \Phi_2] \tag{13}$$

A general wave function for an avoided crossing state (ACS) is obtained by mixing in the carbocation configuration, Φ_3 (**3a** or **3b**), with a general mixing coefficient λ, where $[1 + \lambda^2]^{-1/2}$ is the normalization constant. Using this ACS wave function, we

$$\Psi_{ACS} = [1 + \lambda^2]^{-1/2}\{\Phi_{HL} + \lambda\Phi_3\} \tag{14}$$

then choose permissible coefficients (a_i') of the three contributing VB configurations, and charge distributions that are consistent with the avoided crossing constraint (eq 14). These guess coefficients and charges can serve then to assess the "distance" of the ACS wave function (eq 14) from the actual computed TS wave function.

Table 11. Computed MP2 TS Group Charges[a] and Best Fit ACS Group Charges[b] for S_N2 Reactions

reaction		group charges			λ^2 [b]	$\Delta \times 10^{-3}$ [c]
		Br	CH_3	I		
Br···CH_3···I	TS	−0.62	0.16	−0.54		
	ACS	−0.58	0.16	−0.58	~0.18–0.19	1.764
		Cl	CH_3	Br		
Cl···CH_3···Br	TS	−0.66	0.22	−0.56		
	ACS	−0.61	0.22	−0.61	~0.27–0.28	3.295
		Cl	CH_3	I		
	TS	−0.62	0.16	−0.54		
Cl···CH_3···I	ACS	−0.58	0.16	−0.58	0.19	9.409[e]
	ACS	−0.59	0.18	−0.59	0.23	9.409[e]
		NH_3	CH_3	I		
H_3N···CH_3···I	TS	0.33	0.28	−0.61		
	ACS	0.36	0.28	−0.64	~0.39–0.40	1.225
		NH_3	CH_3	Br		
H_3N···CH_3···Br	TS	0.34	0.30	−0.65		
	ACS	0.35	0.30	−0.65	~0.43–0.45	0.036
		NH_3	CH_3	Cl		
H_3N···CH_3···Cl	TS	0.36	0.33	−0.68		
	ACS	0.34	0.32	−0.66	~0.46–0.48	0.729
		NH_3	CH_3	Br		
H_3N···CH_3···Br	TS[d]	0.27	0.46	−0.73		
	ACS	0.27	0.46	−0.73	0.85	0.033

[a] TS charges obtained at the MP2//MP2 level. [b] Best fit ACS charges obtained from λ^2 of the best fit Ψ_{ACS} (eq 14). [c] Residual in 10^{-3} units defined by eq 20. [d] Values refer to the TS of Bertran et al. (ref 17). The charges in ref 17 were obtained at the SCF level with the 3-21G basis set. [e] These two wave functions possess the same residuals.

The group charges for an ACS are given by eq 15 for the ionic TSs and by eq 16 for the Menschutkin TSs:

$$Q(Y) = Q(X) = -(0.5 + \lambda^2)/(1 + \lambda^2); \quad Q(R) = \lambda^2/(1 + \lambda^2) \tag{15}$$

$$Q(NH_3) = 0.5/(1 + \lambda^2); \quad Q(X) = -(0.5 + \lambda^2)/(1 + \lambda^2); \quad Q(R) = \lambda^2/(1 + \lambda^2) \tag{16}$$

The corresponding allowed VB coefficients for both cases are given by eq 17 and 18:

$$a_1' = a_2' = 1/[2(1 + \lambda^2)]^{1/2} \tag{17}$$

$$a_3' = \lambda/(1 + \lambda^2)^{1/2} \tag{18}$$

On the basis of these expressions one can proceed to find the guess ACS wave function of best fit to the TS wave function. The best fit is searched for in three different ways: (i) by linear regression between the TS charges (Tabels 5, 6) and the charges of the ACS wave function (eqs 15, 16); (ii) from the overlap (eq 19) of the TS wave function, with coefficients a_i (eq 6), and the guess wave functions, with coefficients a_i' (eqs 17, 18); and (iii) from the "distance" between the wave functions, defined by the residual, Δ, of the coefficients in eq 20. By comparison of the three fitting procedures, we were able to define for each TS a common best fit ACS.

$$S = \langle\Psi_{TS}|\Psi_{ACS}\rangle = \sum_i a_i a_i'; \quad i = 1\text{–}3 \tag{19}$$

$$\Delta = \sum_i (a_i - a_i')^2; \quad i = 1\text{–}3 \tag{20}$$

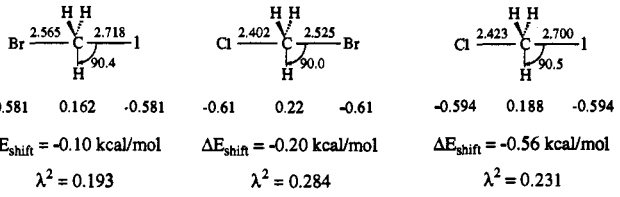

Figure 4. ACS structures for the ionic S_N2 reactions obtained by use of the reaction vector methodology.

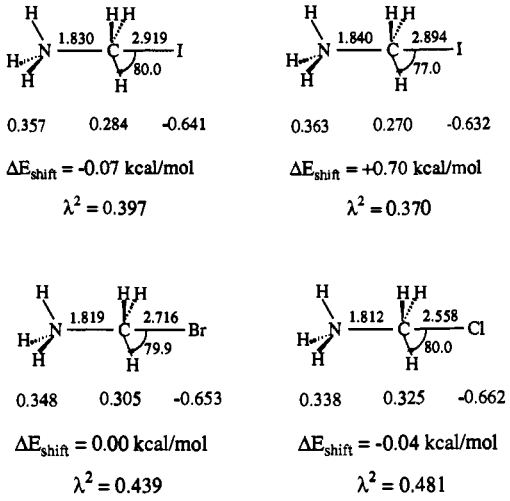

Figure 5. ACS structures for the Menschutkin S_N2 reactions.

Table 11 shows the charge distributions of the ACS with the best fit wave function to the TS, along with the computed TS charges at the consistent MP2//MP2 level. Since the residual appears to be the most sensitive criterion for the quality of the fit, these values are also reported in the table. Inspection of Table 11 reveals that in each case the fitted ACS charge distribution (labeled ACS) is quite close to the TS one (labeled TS), the largest deviations being 0.05*e*. It is interesting to note that in the ionic cases the fitted charges are simply the average of the X and Y charges in the actual TSs. For the Menschutkin TSs, the quality of the fit is extremely good and in some cases the fit is virtually perfect. We conclude therefore *that the ACS wave function is an excellent approximation for the TS wave function.*

Three-Dimensional Search for Avoided Crossing Structures. We begin our search for ACS structures from the TS structure and change its geometry gradually in order to find a three-dimensional structure that possesses a charge distribution that matches that of the ACS wave function (eq 14). Once such a structure is found, we can then assess the geometric and energetic shifts of the ACS from the actual TS. In addition, the ACS wave functions found in this way can then be compared to the best fit ACS wave functions listed Table 11, to test for consistency.

From the data in Table 11, it is apparent that in order to obtain the ACS charge distribution from the TS charge distribution, some charge (0.01–0.05*e*) needs to be transferred from the nucleophile to the leaving group. From the discussion of the charge–geometry dependence in **7** and **8**, it is apparent that in order to induce the requisite charge transfer and thereby achieve the ACS, the three-dimensional structure of the reaction complex must be changed parallel to the reaction coordinate motion, as indicated in **7**. This is the basis of the search strategy which is described in the computational section as the "reaction vector methodology" and in which the ACS is sought by stepping along the reaction vector in the direction indicated initially by the required direction of charge transfer (depicted in **7** and **8**).

Figure 4 shows the located ACS geometries for the ionic S_N2 reactions, while Figure 5 shows those geometries for the Menschutkin reactions. In each case, the structures are depicted along with their charge distributions, their λ^2 value according to the ACS wave function in eq 14, and the energy shift relative to the corresponding TS. A comparison of the λ^2 values of the located ACSs with the corresponding values of the best fit procedure in Table 11 shows that the two sets of λ^2 values obtained by the two independent methods are remarkably close; in fact they are virtually identical. This excellent agreement reaffirms the validity of the search methodology.

Figure 5 contains two ACS candidates for the Menschutkin reaction of CH_3I. The right-hand side structure is obtained by a geometric grid about the TS and qualifies as the point with the charge distribution satisfying the ACS wave function with $\lambda^2 = 0.370$. This ACS is seen to be higher in energy relative to the TS, while all other ACSs which are obtained by use of the reaction vector methodology are lower in energy than their corresponding TSs. Thus, while all the ACSs which are lower than the TS lie parallel to the "reaction coordinate", the $NH_3\cdots CH_3\cdots I$ ACS with $\Delta E_{shift} > 0$ lies in a perpendicular direction to the "reaction coordinate." Given the much smaller absolute value of ΔE_{shift} in the parallel direction, it is apparent, at least from this case, that the reaction vector methodology locates an ACS which is a better approximation for the TS than the "perpendicular" ACS. We are therefore dealing with ACSs which lie along the "reaction coordinate" and adjacent to the TS.

How close are the ACSs to their corresponding TSs? In terms of bond lengths the two structural types are very similar. The bond lengths differ by 1.5–3.8% for the ionic TSs and by 0.22–1.8% from the Menschutkin TSs. In the case of $NH_3\cdots CH_3\cdots Br$, the ACS bond lengths deviate by 0.22% and 0.41%, respectively, relative to the TS, so here the two structures are virtually identical. The largest deviation is exhibited by the $Cl\cdots CH_3\cdots I^-$ ACS, whose structure differs by 3.6% (in the C–Cl bond) and 3.8% (in the C–I bond) relative to the corresponding TS. Although the deviation in this case is somewhat larger, it is fair to conclude that here also the TS and ACS are in close proximity to one another.

Another criterion for the similarity of the two structures is the relative energy of the ACS and the corresponding TS. This comparison further strengthens the conclusion drawn from the structural comparison. Thus, out of the six ACSs located by the reaction vector methodology the energy of five differ from the corresponding TS by less than 0.20 kcal/mol, while the sixth one differs by 0.56 kcal/mol. For the Menschutkin ACSs the agreement is even better; all lie within 0.1 kcal/mol of their corresponding TS, so that the two sets of structures are therefore essentially identical in energy. The conclusion is apparent: the TS is situated in the immediate vicinity of the avoided crossing point, so that *the ACS may be taken as an extremely good approximation for the TS*. Both lie in a region that we might call the *transition state region.*

C. Implications of the TS Paradigm. The charge distribution within an S_N2 transition state is conventionally considered to provide information regarding the position of the TS along the reaction coordinate. Consider for example the charge distribution of the Menschutkin S_N2 TSs in Table 6. It can be seen that the NH_3 group carries a small positive charge, while the X group carries a large negative charge, more than double in absolute value. According to the conventional wisdom, this TS would be described as "early" with respect to the degree of charge transfer from the nucleophile (NH_3), but as "late" with respect to the charge development on the leaving group. This was the conclusion drawn by Arnett and Reich[22a] in their extended rate–equilibrium study of the Menschutkin reaction, although aspects of their analysis were subject to some criticism.[5b,22b,c] However the question that arises is what is the significance of a transition state that is early with respect to one molecular parameter but late with respect to another? And what are the implications of such

behavior to general TS concepts, such as the Leffler–Hammond postulate? The VB analysis (Table 11 and Figure 5) shows that this seemingly contradictory charge development in the Menschutkin TSs is a simple outcome of the electronic structure imposed on the TS by the neighboring ACS.

Modeling the TS in terms of an ACS provides therefore new insight into the field of TS structure. Firstly, the TS paradigm demonstrates that the geometry of the TS is located very near or directly on the seam of avoided crossing of the reactant and product HL configurations (the HL state is eq 13).[46,47] On the other hand, TS charge distribution is found to depend on the proportion of the intermediate configurations which mix into the HL state. Thus, while the TS geometry behaves effectively as a two-configuration property,[46] the charge distribution of the TS behaves differently and is explicitly a many-configuration property. It follows, therefore, that the commonly accepted link between TS geometry and charge distribution will often break down. *Thus, TS charges should not be used generally to assess the geometric "earliness" or "lateness" of the TS.*

Secondly, the correlation between TS geometry and exothermicity, noted by Wolfe, Mitchell, and Schlegel[12] and by Shaik, Schlegel, and Wolfe,[42b] and the *absence* of a correlation between TS charge and exothermicity[11] may have a simple origin. TS geometry and exothermicity correlate because it is the product HL configuration that affects both the geometry of intersection and the exothermicity. In other words the Leffler–Hammond idea holds for geometry; within a related family, more exothermic processes *are* expected to be more reactant-like in geometric terms. However, TS charge depends strongly on the contribution of the intermediate configurations to the TS wave function. Since the extent of mixing of these configurations *into the TS* is not directly linked to reaction exothermicity, the lack of a general correlation between TS charge and exothermicity is not surprising. Similar conclusions were reached by Bertran et al.[17] based on their findings that solvent polarity affected the position of the TS differently than its charge distribution.

Conclusions

This work investigates the transition states (TSs) for the ionic and Menschutkin S_N2 reactions of CH_3X (X = Cl, Br, I) derivatives and demonstrates that the TSs may be approximated by electronic states termed avoided crossing states (ACSs). Methodologies are described for finding the ACS with the best fit to the TS, in terms of wave function and charge distribution, and for finding the ACS three-dimensional structure.

The study demonstrates that the TSs of the target S_N2 reactions are very well approximated by ACSs. The TSs that we have examined cover a wide range of reaction energy (over 100 kcal/mol) and are structurally varied both in reaction type (ionic and Menschutkin reactions) and in atomic identity (NH_3, Cl, Br, and I). Moreover, while some of the structures can be considered "early" (less deformed) and others very "late" (the very deformed Menschutkin TSs), all conform to a single description; they are all anchored very closely to an ACS which lies nearby along the reaction coordinate. The work thus provides a link between the formal mathematical definition of a TS as a saddle point and its chemical description in terms of electron distribution and reorganization. Thus, the ACS concept is not designed to replace the mathematical definition of the TS, but rather to complement it with the missing chemical model.

Because the ACS has a well-defined electronic VB structure (defined by eq 14), some of the vagueness associated with descriptions of the TS can be eliminated. Since the ACS is demonstrated to be reasonably close to the actual TS in structure, energy, and electronic distribution, it has considerable merit as a reference point for the TS over other points of reference (such as reactants and products) along the reaction coordinate. We conclude, therefore, that *the ACS can serve as a useful transition-state paradigm in chemical reactivity.*

A key feature of the ACS paradigm is that it breaks the widely accepted linkage between TS charge and geometry implicit in existing TS models. While TS geometry is found to depend on reaction exothermicity, in line with the Leffler–Hammond postulate, TS charge is largely governed by the extent of mixing of an intermediate configuration into the TS wave function and is *not* related in a simple linear fashion to the geometric position of the TS along the reaction coordinate. This conclusion would appear to reaffirm the need to continue the reevaluation of the traditional physical organic perspective on structure–reactivity relationships.[5,14]

Finally, we should point out that in certain extreme cases one might expect the ACS paradigm to break down. If the mixing of the intermediate configuration is particularly large, then the TS may be displaced away from the ACS. For the S_N2 systems studied here this was not observed, but one cannot rule out the possibility that this will not occur in other systems. Hence, it would be desirable to explore to what extent the ACS approximation holds for other reaction types and for reactions in solution.[48] Some of these studies are already in progress.

Acknowledgment. This research carried out at The Hebrew University is supported in part by the Basic Research Fund administered by the Academy of Sciences and Humanities and in part by the Ministry of Science and Technology (MOST) of Israel. A.I. thanks MOST, the Ministry of Absorption, and the Wolfson Foundation for the fellowships which enables his participation in the research, and A.P. thanks the Australian Research Council for the award of a Senior Research Fellowship.

(46) Note that the precise location of the TS on the seam of the HL state may well depend on the intermediate configurations. However, this is not an explicit effect as that on the charge distribution.

(47) For a recent use of reactant and product surface crossing in molecular mechanics modeling of reactivity, see: Jensen, F. *J. Am. Chem. Soc.* **1992**, *114*, 1597.

(48) Current quantum chemistry programs (e.g., GAUSSIAN-92; GAMESS-92) are equipped with solvation codes which allow the TSs to be placed in solvation environments.